

# The Surface Structure of Sulfated Zirconia: Periodic ab Initio Study of Sulfuric Acid Adsorbed on ZrO<sub>2</sub>(101) and ZrO<sub>2</sub>(001)

Frank Haase\* and Joachim Sauer

Contribution from the Institut für Chemie, Humboldt-Universität Berlin, Jägerstrasse 10/11, D-10117 Berlin, Germany

Received July 20, 1998. Revised Manuscript Received October 19, 1998

**Abstract:** Periodic plane wave pseudopotential calculations based on density functional theory are performed to reveal the structure of sulfur species on the surface of tetragonal zirconia. The most stable configurations found are a tridentate sulfate anion on the (101) surface and an SO<sub>3</sub> complex on the (001) surface which is also 3-fold coordinated but unlike the sulfate anion is bonded to the surface via two oxygen atoms and the sulfur atom. The adsorption energies of these tridentate complexes are -322 kJ/mol for the former and -467 kJ/mol for the latter structure. On the (001) surface we also identified a bidentate sulfate complex as a stable structure with an adsorption energy of -408 kJ/mol. However, as MD simulations at a temperature of 800 K show, this bidentate configuration is transformed into a 3-fold coordinated structure accompanied by a reconstruction in the oxygen top layer. The observed IR spectra can be explained by the presence of sulfate anions on both crystallographic planes studied in this work. The calculated vibrational frequencies of the two tridentate surface complexes exhibit a gap of about 360 cm<sup>-1</sup> between the  $\nu(\text{S}=\text{O})$  and  $\nu(\text{S}-\text{O})$  stretching bands, which agrees well with experimental IR spectra of sulfated zirconia samples calcined at about 900 K. For the bidentate sulfate complex as well as for a less stable hydrogen sulfate anion we calculate  $\nu(\text{S}-\text{O})$  stretching frequencies in the range 1250–900 cm<sup>-1</sup> which qualitatively explain the observed IR spectra of sulfated zirconia samples calcined at 800 K. On the basis of the calculated deprotonation energies, which are in the range 1350–1550 kJ/mol, we conclude that the hydroxyl groups on the two surfaces studied are less acidic than bridged hydroxyls in zeolites, regardless of the presence or absence of sulfate anions. The -1170 kJ/mol proton affinity of oxygen atoms on the (001) surface indicates that the zirconia surface is a strong base. This result and our finding of a strong electrostatic interaction with the surface explain why adsorbed sulfuric acid is completely deprotonated.

## 1. Introduction

In 1980 Hino et al.<sup>1</sup> reported that the surface of zirconium dioxide, when treated with sulfuric acid, exhibits unique activity in the catalytic isomerization of hydrocarbons. Because the product distribution was typical of paraffin isomerization by sulfuric acid and the reaction temperature was remarkably low, it was concluded that sulfated zirconia (SZ) can be considered as a solid superacid or at least as a very strong solid acid. This has triggered a multitude of studies, and whether superacidity applies to SZ is still subject to debate. While earlier studies supported superacidity as the primary source of the catalytic activity,<sup>2,9</sup> there is growing evidence that this might not be the

case.<sup>3–5</sup> As to the crystal phase, it seems to be generally accepted that a stable tetragonal phase is a necessary condition to obtain catalytically active samples.<sup>8</sup> Sulfated monoclinic zirconia develops virtually no activity in hydrocarbon isomerization reactions.

To provide information about the structure of the sulfur surface species, a variety of spectroscopic and surface sensitive techniques were applied. On the basis of IR and X-ray photoelectron spectroscopy (XPS) results, Yamaguchi et al.<sup>2</sup> suggested a surface sulfate species containing a O=S=O moiety doubly coordinated (bidentate) to the zirconia surface, **1c**. Later, Bensitel et al.<sup>6</sup> produced evidence for the existence of two structures at moderate coverage which possibly reside on different crystal planes.<sup>7</sup> Both species contain only one S=O bond and are coordinated to surface zirconium atoms via three S–O bonds, **1a**. Riemer et al.<sup>9</sup> agreed with a tridentate surface sulfate species containing just one S=O bond. However, they suggested a HSO<sub>4</sub><sup>-</sup> group being present at the surface, **1b**, because they observed an O–H stretching band at 3650 cm<sup>-1</sup> which was not present on the sulfate-free material. Furthermore, such a structure could explain the observed high <sup>1</sup>H NMR shift of 5.85 ppm. These conclusions were supported by Adeeva et al.<sup>5</sup> and Kustov et al.,<sup>10</sup> who proposed a similar model in which the SOH group is H-bonded to a surface oxygen or an internal

(1) Hino, H.; Kobayashi, S.; Arata, K. *J. Am. Chem. Soc.* **1979**, *101*, 6439. Hino, H.; Arata, K. *J. Chem. Soc., Chem. Commun.* **1980**, 851.

(2) Yamaguchi, T.; Jin, T.; Tanabe, K. *J. Phys. Chem.* **1986**, *90*, 3148. Jin, T.; Yamaguchi, T.; Tanabe, K. *J. Phys. Chem.* **1986**, *90*, 4794.

(3) Morterra, C.; Cerrato, G.; Bolis, V.; Di Ciero, S.; Signoreto, M. *J. Chem. Soc., Faraday Trans.* **1997**, *93*, 1179.

(4) Drago, R.; Kob, N. *J. Phys. Chem. B* **1997**, *101*, 3360.

(5) Adeeva, V.; de Haan, J. W.; Jänchen, J.; Lei, G. D.; Schünemann, V.; van de Ven, L. J. M.; Sachtler, W. M. H.; van Santen, R. A. *J. Catal.* **1995**, *151*, 364.

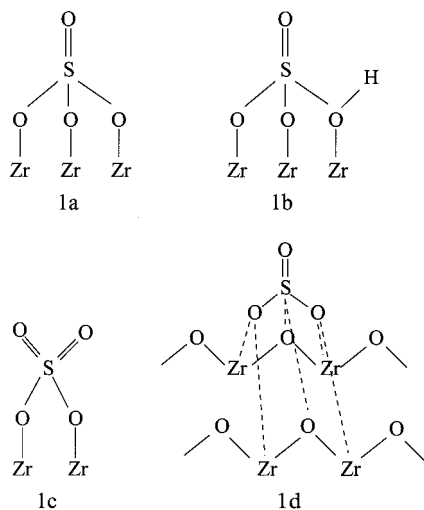
(6) Bensitel, M.; Saur, O.; Lavalley J.-C.; Morrow, B. A. *Mater. Chem. Phys.* **1988**, *19*, 147.

(7) According to Morterra et al.<sup>8</sup> the crystal phase of the samples used by Bensitel et al. was mainly monoclinic.

(8) Morterra, C.; Cerrato, G.; Pinna, F.; Signoreto, M. *J. Catal.* **1995**, *157*, 109.

(9) Riemer, T.; Spielbauer, D.; Hunger, M.; Mekhemer, G. A. H.; Közinger, H. *J. Chem. Soc. Chem. Commun.* **1994**, 1181.

(10) Kustov, L. M.; Kazansky, V. B.; Figueras, F.; Tichit, D. *J. Catal.* **1994**, *150*, 143.

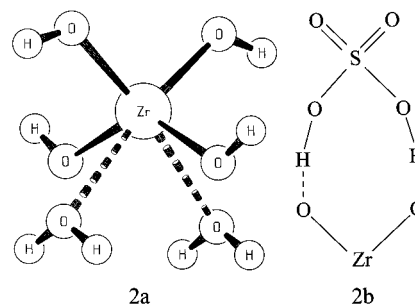


H-bond to a sulfate oxygen is formed. White et al.<sup>11</sup> suggested an  $\text{SO}_3$  molecule adsorbed on the (001) plane of tetragonal zirconia in which the sulfur interacts with five different oxygen atoms and which has only one  $\text{S}=\text{O}$  bond, **1d**. Finally, Babou et al.<sup>12</sup> assumed as many as four different surface species ( $\text{SO}_3$ ,  $\text{H}_2\text{SO}_4$ ,  $\text{HSO}_4^-$ , and  $\text{SO}_4^{2-}$ ) depending on the dehydration state of the sample.

While the above studies applied spectroscopic techniques which only provide indirect information on the structure of the surface sulfate species, Benaissa et al.<sup>13</sup> applied high-resolution transmission electron microscopy (HRTEM), which should allow a direct observation of the surface sulfate complexes. However, the image contrast was not sufficient and they were not able to discriminate between the bidentate and tridentate structure types discussed above. The authors suggest that the (110) plane is preferably formed on sulfation and that its structure is appropriate to accommodate sulfate groups in the 2- or 3-fold coordination. In another work<sup>14</sup> it was found that tetragonal samples of SZ stabilized by Fe/Mn additionally exhibit (101) and (001) facets as well, an observation also made by Morterra et al.<sup>15</sup>

Despite the great deal of experimental work, no clear picture about the structure of surface sulfur species emerged. In such a situation quantum mechanical methods can be very helpful, provided that the computational technique is reliable and the models used are adequate. They can predict structures of different surface species and show which spectroscopic signals can be assigned to a given species. They also facilitate our understanding of how and why certain surface species form. A common approach to the surface problem is the cluster model.<sup>16</sup> It cuts out the local site of interest of the solid catalyst together with some part of its environment, saturates the dangling bonds with hydrogen atoms, and treats the entire system as a molecule. Quantum chemical methods up to high levels of sophistication can be applied depending on the size of the model system. Babou et al.<sup>30</sup> used this approach to model different sulfate

species on the surface of zirconia. A cluster comprising a  $\text{Zr}(\text{OH})_4$  tetrahedron and two additional water molecules was selected as a model of the (001) surface of zirconia, **2a**. As the most stable surface complex, a sulfuric acid molecule strongly H-bonded to the zirconia oxygen atoms was predicted, **2b**.



However, as we will show in this work, at moderate coverage a sulfuric acid molecule does not exist on the (001) plane of zirconia, H-bonded or interacting in any way whatsoever. Furthermore, the chosen cluster does not allow one to mimic a 2- or 3-fold coordination of a sulfate species to the zirconia surface and hence is not suited to examine the structure proposals that emerged from experimental studies.

We therefore decided to follow the alternative approach and to apply periodic boundary conditions. Though periodic methods based on density functional theory (DFT) together with a plane wave basis set are widely and successfully applied in theoretical surface physics<sup>24–26</sup> especially in studies on metal oxides,<sup>27</sup> no study was published yet on SZ. In this work we study the interaction of sulfuric acid with the surface of tetragonal zirconia. To our knowledge this study is the first on SZ which uses a realistic model of the surface of tetragonal zirconia together with ab initio methods. The present work aims at predicting structures of surface sulfur species that are in accord with the experimental evidence available. Although the unique catalytic activity of SZ is often ascribed to the simultaneous presence of both Brønsted and Lewis sites,<sup>3,28</sup> in this paper we restricted the discussion of acidic properties to Brønsted acidity. A detailed analysis of the strength of the Lewis sites on the surface of pure zirconium oxide as well as of the sulfated material will be the subject of a forthcoming paper. As IR spectroscopy is the most frequently applied technique, we also carried out calculations of vibrational frequencies. Because there is still no information available concerning which crystallographic plane is involved in the catalytic process, we first studied the relative stability of different surfaces and then investigated the adsorption of sulfuric acid on the two most

(11) White, R. L.; Sikabwe, E. C.; Coelho, M. A.; Resasco, D. E. *J. Catal.* **1995**, *157*, 755.

(12) Babou, F.; Coudurier, G.; Vadrine, J. *J. Catal.* **1995**, *152*, 341.

(13) Benaissa, M.; Santiesteban, J. G.; Diaz, G.; Chang, C. D.; Jose-Yacamán, M. *J. Catal.* **1996**, *161*, 694.

(14) Benaissa, M.; Santiesteban, J. G.; Diaz, G.; Jose-Yacamán, M. *Surf. Sci.* **1996**, *364*, L591.

(15) Morterra, C.; Cerrato, G.; Ferroni, L.; Montanaro, L. *Mater. Chem. Phys.* **1994**, *37*, 243.

(16) Sauer, J. *Chem. Rev.* **1989**, *89*, 199.

(17) Bolis, V.; Magnacca, G.; Cerrato, G.; Morterra, C. *Langmuir* **1997**, *13*, 888.

(18) Sauer, J. *J. Mol. Catal.* **1989**, *54*, 312.

(19) Brändle, M.; Sauer, J. *J. Am. Chem. Soc.* **1998**, *120*, 1556.

(20) Hill, J.-R.; Sauer, J. *Chem. Phys. Lett.* **1994**, *218*, 333.

(21) Haase, F.; Sauer, J. To be published.

(22) Aue, D. H.; Bowers, M. T. In *Gas-Phase Ion Chemistry*; Bowers, M. T., Ed.; Academic Press: New York, 1979; Vol. 2, pp 1–51.

(23) Pauling, L. *The Nature of the Chemical Bond*; Cornell University Press: New York, 1960.

(24) Remler, D. K.; Madden, P. A. *Mol. Phys.* **1990**, *70*, 921.

(25) Galli, G.; Parrinello, M. In *Computer Simulations in Material Science*; Meyer, M.; Poutikis, V., Eds.; Kluwer Academic Publishers: Dordrecht, 1991, pp 283–304.

(26) Payne, M. C.; Teter, M. P.; Allen, D. C.; Arias, T. A.; Joannopoulos, J. D. *Rev. Mod. Phys.* **1992**, *64*, 1045.

(27) Lindan, P. J. D.; Harrison, N. M.; Gillan, M. J. *Phys. Rev. Lett.* **1998**, *80*, 762.

(28) Clearfield, A.; Serrette, G. P. D.; Khazi-Syed, A. H. *Catal. Today* **1994**, *20*, 295.

(29) Babou, F.; Bigot, B.; Sautet, P. *J. Phys. Chem.* **1993**, *97*, 11501.

(30) CPMD Version 3.0, J. Hutter, P. Ballone, M. Bernasconi, P. Focher, E. Fois, St. Goedecker, M. Parrinello, M. Tuckerman, MPI für Festkörperforschung Stuttgart und IBM Research 1990–1996.

stable surfaces, (101) and (001). Molecular dynamics (MD) simulations proved very useful as they allow the exploration of larger parts of the configuration space than the usual relaxation methods. This feature is essential for systems that have many minima and therefore many different local structures. Because sulfuric acid is one of the strongest acids known and the zirconia surface contains, besides Lewis sites, basic sites represented by the coordinatively unsaturated oxygen atoms, the interaction between sulfuric acid and zirconia can be understood in terms of acid–base reactions. In contrast to such reactions in solution, in this heterogeneous reaction the sulfate ions bind in many different ways to the solid surface depending on the particular topology of the surface. We will show below that the reactivity of SZ and the structure of the surface complexes can be explained if both the acid–base properties of the reaction partners and the topologies of the different surfaces are taken into account.

## 2. Computational Details

Two types of DFT calculations were performed: structure relaxations in combination with molecular dynamics (MD) simulation and harmonic frequency calculations. We used the CPMD program<sup>30</sup> with its message passing parallelized implementation on CRAY T3E computers. The gradient-corrected functional of Perdew, Burke, and Ernzerhof (PBE)<sup>31</sup> was employed in the calculation of the exchange–correlation energy. The PBE functional originates from the Perdew and Wang functional<sup>32–34</sup> and gives essentially the same results but has some improved features such as the smoother potential and the significantly simpler formulation. Only the valence electrons were treated explicitly. The atomic cores were represented by pseudopotentials which were constructed by *ab initio* DFT atomic calculations. While for Zr a norm-conserving pseudopotential was generated according to Martins and Troullier,<sup>35</sup> for all other elements (H, C, O, S) the supersoft scheme of Vanderbilt<sup>36</sup> was employed. The Vanderbilt pseudopotentials for C, O, and S were generated using two construction energies per angular momentum with core cutoff radii of 1.3, 1.4 and 1.45 au, respectively. For H, one reference energy (1s eigenvalue) for the *s* angular momentum channel was employed and a core radius of 0.7 au was used. The Martins–Troullier pseudopotential of Zr was generated from the  $4d^2 5s^1 5p^0$  atomic valence configuration with the following core cutoff radii:  $r_C^d = 2.45$ ,  $r_C^s = 2.85$ , and  $r_C^p = 3.15$  au. The *s* component was selected as local potential. Brillouin zone sampling was done only at the  $\Gamma$  point.

## 3. Test Calculations

To assess the accuracy of the adopted method and to establish a sufficiently converged kinetic energy cutoff up to which all plane waves are included in the expansion of the Kohn–Sham orbitals, we first considered the structures of the tetragonal and cubic phases of bulk zirconia. Table 1 summarizes the results obtained for increasing kinetic energy cutoffs ( $K_C$ ). While the unit cell constants of the cubic phase are slightly overestimated, the values for tetragonal zirconia agree very well with experimental results. Moreover, the results for cutoffs of about 30 Ry seem to be already well converged at least for these bulk systems.

To test the accuracy of the pseudopotentials for S, O, and H, a series of structure relaxations on sulfuric acid and sulfur trioxide were performed. In these calculations no periodic boundary conditions were imposed. The CPMD code uses a method similar to that of Barnett and Landman<sup>37–39</sup> which is based on a special algorithm for nonperiodic systems to solve the Poisson equation for the Hartree potential. A cubic

**Table 1.** Equilibrium Cell Constants (pm) of the Cubic and Tetragonal Phase of Bulk  $ZrO_2$  for Increasing Kinetic Energy Cutoffs  $K_C$  (Ry)

$K_C$	fcc	tetragonal	
	<i>a</i>	<i>a</i>	<i>c</i>
25	518.1		
30	518.4	366.1	526.7
35	518.3	366.2	526.5
exptl <sup>a</sup>	509	364	527

<sup>a</sup> Reference 41.

**Table 2.** Selected Structural Parameters (pm and deg) of the Gas-Phase Equilibrium Structures of  $SO_3$  and  $H_2SO_4$  at Various Kinetic Energy Cutoffs  $K_C$  (Ry)

$K_C$	SO <sub>3</sub>	H <sub>2</sub> SO <sub>4</sub>			
	<i>r</i> (S=O)	<i>r</i> (S=O)	<i>r</i> (S–O)	<i>r</i> (OH)	$\angle$ (O=S=O)
25	145.1	144.3	160.7	99.1	124.4
30	145.0	144.2	160.7	98.8	124.4
35	145.0	144.2	160.7	98.8	124.7
40	145.0	144.2	160.7	98.7	124.7
B3LYP/DZP <sup>a</sup>	145.6	144.8	163.1	97.6	125.1
HF/DZP <sup>b</sup>	140.6	141.2	157.2	95.3	123.9
exptl <sup>c</sup>	142.0	142.2	157.4	97.0	123.3

<sup>a</sup> All electron DFT calculation employing the B3LYP functional and a DZP (double-zeta polarization) Gaussian function basis set. <sup>b</sup> All electron Hartree–Fock calculation using a DZP Gaussian function basis set. <sup>c</sup> SO<sub>3</sub>: ref 42. H<sub>2</sub>SO<sub>4</sub>: ref 43.

cell with a length of 18 bohr was adopted, and the molecules were placed at the center of the box. The point groups  $C_2$  ( $H_2SO_4$ ) and  $D_{3h}$  ( $SO_3$ ) were imposed, and cutoffs between 25 and 40 Ry were applied. The results for the structural parameters (Table 2) show a remarkable stability with increasing  $K_C$ . Bond lengths vary by 0.4 pm and bond angles by 0.3° in the range of cutoffs studied. Comparison of the calculated values with experimental microwave data reveals that bond lengths are slightly too large (3.7 pm or 2% for the S–O bond). This deviation is neither due to the plane wave basis set nor caused by the ultrasoft pseudopotentials. Table 2 also shows results obtained by the Hartree–Fock method (HF) and the DFT method using the B3LYP functional. Both calculations treat all electrons explicitly and employ a DZP atom-centered Gaussian basis to expand the orbitals. While the HF method gave results in very good agreement with experiment, the B3LYP DFT calculation, although including the HF exchange in part in the exchange correlation functional, shows the same overestimation of S–O and S=O bond lengths as the plane wave pseudopotential method.

Although the data of Table 2 suggest a converged basis set at 30 Ry, we checked a third convergence criterion: the kinetic energy of the Zr pseudoatom. The latter is a good predictor of the pseudoatom total energy,<sup>40</sup> which in turn controls the convergence of the total energy of the zirconia solid in our case. Good convergence will be achieved if the Fourier transform of the pseudowave function possesses a minimal amount of kinetic energy beyond a given cutoff. For the Zr atom with the chosen norm-conserving pseudopotential, this condition is fulfilled at a cutoff of only 35 Ry. We therefore adopted this cutoff in all the calculations reported below.

To model a crystal surface which lacks periodicity perpendicular to the surface, one has to resort to the supercell method. An appropriate supercell comprises a slab which is thick enough to prevent the two

(31) Perdew, J. P.; Burke, K.; Ernzerhof, M. *Phys. Rev. Lett.* **1996**, *77*, 3865.

(32) Perdew, J. P.; Wang, Y. *Phys. Rev. B* **1986**, *33*, 8800.

(33) Perdew, J. P.; Chevary, J. A.; Vosko, S. H.; Jackson, K. A.; Pederson, M. R.; Singh, D. J.; Fiolhais, C. *Phys. Rev. B* **1992**, *46*, 6671.

(34) Perdew, J. P. *Phys. Rev. B* **1986**, *33*, 8822.

(35) Troullier, N.; Martins, J. L. *Phys. Rev. B* **1991**, *43*, 1993.

(36) Vanderbilt, D. *Phys. Rev. B* **1990**, *41*, 7892.

(37) Barnett, R. N.; Landman, U. *Phys. Rev. B* **1993**, *48*, 2081.

(38) Hockney, R. W. *Methods Comput. Phys.* **1970**, *9*, 136.

(39) Eastwood, J. W.; Brownrigg, D. R. K. *J. Comput. Phys.* **1979**, *32*, 24.

(40) Rappe, A. M.; Joannopoulos, J. D. In *Computer Simulations in Material Science*; Meyer, M., Poutikis, V., Eds.; Kluwer Academic Publishers: Dordrecht, 1991; pp 409–422.

(41) Teufer, G. *Acta Crystallogr.* **1962**, *15*, 1187.

(42) Kaldor, A.; Maki, A. G. *J. Mol. Struct.* **1973**, *15*, 123.

(43) Lide, D. R., Ed. *CRC Handbook of Chemistry and Physics*, 64th ed.; CRC Press Inc.: Boca Raton, 1983–1984.



**Table 3.** Equilibrium Surface Energies  $S$  ( $\text{J}/\text{m}^2$ ) of the (101) and (001) Surfaces of Tetragonal Zirconia with Increasing Numbers of  $\text{ZrO}_2$  Layers

no. of layers	$S$	
	(101)	(001)
2	1.142	1.754
3	1.144	1.848
4	1.090	1.882
5	1.045	1.892

surfaces from interacting through the solid and a vacuum region wide enough to avoid interaction with the periodic images of the two surfaces. To set up such a supercell, we carried out several calculations on clean zirconia slabs with increasing numbers of  $\text{ZrO}_2$  layers and monitored the convergence of the surface energy as a very subtle measure of the quality of the slab model. As surface unit cells for the (101) and (001) slab models we chose a  $p(2 \times 1)$  cell with dimensions  $7.32 \times 6.41 \text{ \AA}$  ( $2a \times (a^2c^2)^{1/2}$ ) and a  $p(2 \times 2)$  cell with dimensions  $7.32 \times 7.32 \text{ \AA}$  ( $2a \times 2a$ ), respectively. These parameters were derived from the relaxed tetragonal bulk unit cell of zirconia described above. The dimension in the  $z$ -direction perpendicular to the respective plane is  $30 \text{ \AA}$ . However, in the calculations with adsorbed species we use an increased value of  $35 \text{ \AA}$ . While in these surface energy calculations the slabs were fully relaxed, in the adsorption studies only the first two  $\text{ZrO}_2$  layers were allowed to move freely. Table 3 shows the convergence behavior of the surface energy with respect to the number of  $\text{ZrO}_2$  layers.

It can be concluded that the calculated surface energies of both slab models are well converged at a thickness of 4  $\text{ZrO}_2$  layers. For the 5-layer slab the surface energy is stationary within less than  $0.05 \text{ J}/\text{m}^2$ . In all the slab calculations reported in this work such a 5-layer slab was adopted.

## 4. Results and Discussion

**4.1. Surface Energies.** From the surface energies determined, it follows that the (101) surface is more stable than the (001) surface. To establish a more complete morphology we also computed the energies of the (111) and (100) surfaces with the largest slab model including 5  $\text{ZrO}_2$  layers. The values of  $2.091$  and  $2.272 \text{ J}/\text{m}^2$  for the (111) and (100) surfaces, respectively, indicate that indeed the (101) surface is the most stable one for pure tetragonal zirconia. This conclusion is corroborated by the HRTEM study of Benaissa et al.,<sup>13</sup> who observed long (101) plane terminations, although they characterized their material as a mixture of tetragonal and monoclinic zirconia. Furthermore Morterra et al.<sup>15</sup> studied zirconia of which the tetragonal phase was stabilized by doping with  $\text{Y}_2\text{O}_3$ . Their conclusion was that material calcined at sufficiently high temperature exhibits mainly (101) planes, while at lower calcination temperatures the (111) plane is frequently observed.

**4.2. Structure of Clean Surfaces.** First, we performed structure relaxations of the clean (101) and (001) surfaces of tetragonal zirconia. Analysis of the coordination numbers of the surface oxygen and zirconium atoms reveals that on the (101) surface O sites are 3-fold and the Zr sites are 7-fold coordinated while on the (001) surface these atoms have one coordination less, i.e., they are 2-fold and 6-fold coordinated. No reconstruction was observed for both surfaces, and even relaxation effects are moderate. So the greater stability of the (101) surface can be solely attributed to the higher coordination of the surface zirconium and oxygen atoms. Furthermore at this surface we can identify two different kinds of zirconium sites. In the bulk phase each Zr atom is surrounded by eight oxygen atoms forming two tetrahedra, one with short Zr–O bonds ( $2.15 \text{ \AA}$ , this work) and one with long Zr–O bonds ( $2.37 \text{ \AA}$ , this work). When the crystal is cut along the (101) surface, long as

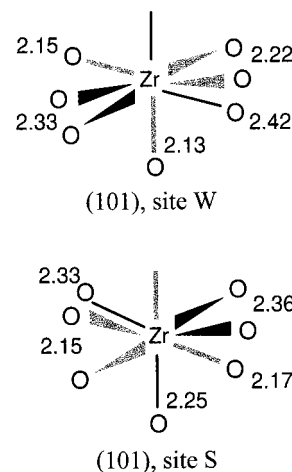


**Figure 1.** Schematic representation of the two possible Zr sites on the  $\text{ZrO}_2(101)$  plane. Solid lines depict tetrahedra with formerly long Zr–O bonds in the bulk system while gray lines depict those built up of short Zr–O bonds (see explanation in section 4.2). Bond lengths are given in angstroms.

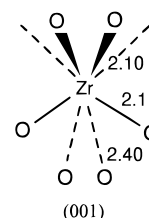


**Figure 2.** Sketch of the coordination of Zr sites on the  $\text{ZrO}_2(001)$  plane. Solid lines represent tetrahedra with short Zr–O bonds in the bulk phase while dashed lines represent tetrahedra with long Zr–O bonds. Bond lengths are given in angstroms.

well as short Zr–O bonds are broken. In Figure 1 these two kinds of Zr sites are sketched together with the equilibrium bond lengths. Gray tetrahedra represent the short Zr–O bonds while black tetrahedra depict long Zr–O bonds. The site with a “long” dangling bond (top of Figure 1), which has a complete tetrahedron with short Zr–O bonds and additionally three long Zr–O bonds, is named Zr site W (“weak”). The site with a “short” dangling bond (bottom of Figure 1) consists of a complete tetrahedron with long Zr–O bonds and three short Zr–O bonds and is named Zr site S (“strong”). Relaxation in the plane affects the Zr–O bond lengths at both sites only marginally (from  $-0.04$  to  $+0.07 \text{ \AA}$ ). At site S (because of the lack of one short Zr–O bond) the long Zr–O bond perpendicular to the plane is shortened noticeably by  $0.12 \text{ \AA}$  to  $2.25 \text{ \AA}$ , which reduces the interlayer distance, a well-known effect.

Figure 2 shows the coordination of the surface Zr sites at the (001) plane. Here the long Zr–O bonds are designated by dashed lines. Cutting along this plane yields 6-fold coordinated Zr atoms and 2-fold coordinated O atoms at the surface. Each Zr site comprises a tetrahedron of four short Zr–O bonds and two long Zr–O bonds. Relaxation causes the surface oxygen layer to move inward to the underlying Zr layer while the subsurface oxygen layer moves outward also to the Zr layer. In this way the layered structure of zirconia is enhanced at the surface, while bond lengths within the layers are altered to a rather limited extent.

**4.3. Adsorption of Water.** It is known that under ambient conditions surface hydroxyl groups exist on oxide surfaces. On the surface of sulfated zirconia these hydroxyl groups are known to be stable up to temperatures higher than those needed to decompose the sulfate species ( $973 \text{ K}^{17}$ ). A possible way to

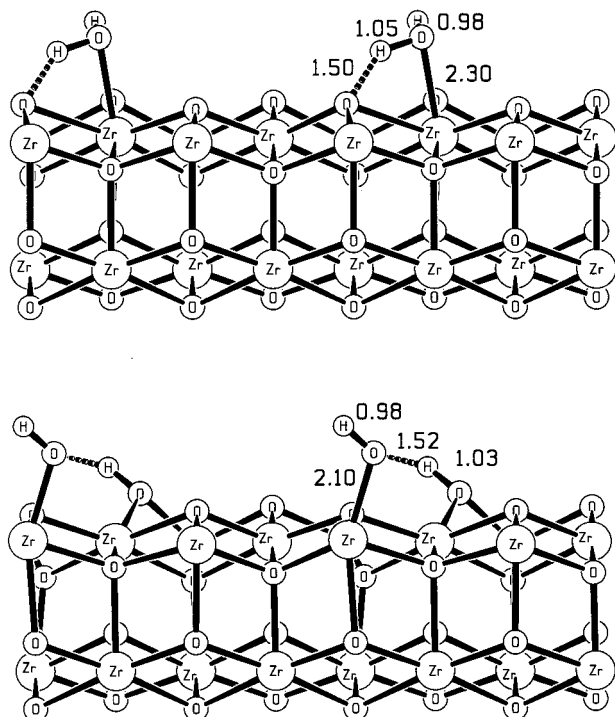


**Figure 3.** Equilibrium structures of the  $\text{H}_2\text{O}/\text{ZrO}_2(101)$  complexes for the two possible Zr sites (see Figure 1). Only the first two  $\text{ZrO}_2$  layers are shown while the unit cell was doubled in the  $x$  direction. Selected bond lengths are given in angstroms.

generate surface hydroxyl groups is the dissociation of adsorbed water molecules on the surface. We therefore performed structure relaxations of adsorbed water on the (101) and (001) surfaces.

Figure 3 shows the first two  $\text{ZrO}_2$  layers of the (101) plane and the two equilibrium structures obtained by adsorbing water at the two possible Zr sites. These two Zr sites interact differently with adsorbed molecules. While on site W, a physisorbed complex forms (top of Figure 3) and water is bound by  $-105$  kJ/mol; on site S, water is chemisorbed and the interaction energy is  $-194$  kJ/mol (bottom of Figure 3). The reason is that the adsorbed water restores the 8-fold coordination of the surface Zr sites. In the physisorption structure it restores a long (weak) Zr–O bond, while in the chemisorption complex a short (strong) Zr–O bond is restored. Consequently, in the physisorption complex the Zr–O bond length of  $2.30$  Å is close to the value of the long Zr–O bond in bulk zirconia ( $2.37$  Å). There is an H-bond interaction of one of the protons with a surface oxygen atom, which causes an elongation of the water O–H bond. On adsorption site S the Zr–OH<sub>2</sub> bond is so strong that the water molecule dissociates. A proton is transferred to a neighboring surface oxygen atom, creating a bridging ZrO(H)Zr hydroxyl group there and leaving a terminal hydroxyl group. The former forms an H bond with the terminal ZrOH group. The Zr–O bond length of the terminal ZrOH group of  $2.10$  Å is even smaller than the corresponding Zr–O bond in bulk zirconia ( $2.15$  Å). Hence, we label the two types of surface Zr sites as “weak” and “strong” Lewis sites, W and S.

On the (001) surface, each Zr site has two “dangling” Zr–O bonds and the adsorbed water molecule interacts with two neighboring Zr atoms, restoring one of the two missing coordinations of each of them. The adsorption is very strong,  $-208$  kJ/mol, comparable to the value calculated for site S on the (101) surface, and water also dissociates (Figure 4). The result is two bridging ZrO(H)Zr groups. One of them (stemming

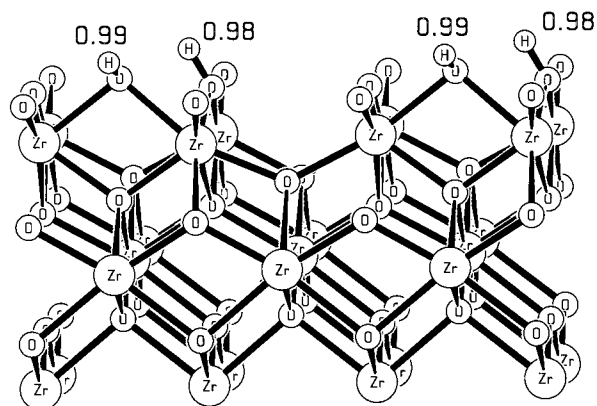
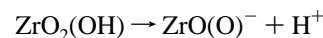


**Figure 4.** Equilibrium structure of the  $\text{H}_2\text{O}/\text{ZrO}_2(001)$  complex. The first three  $\text{ZrO}_2$  layers are shown (which corresponds to one bulk unit cell in the case of the (001) plane) while the unit cell was doubled in the  $x$  direction. Selected bond lengths are given in angstroms.

from the adsorbed water molecule) has two “long” Zr–O bonds, while the other (created by protonation of a surface oxygen atom) has two “short” Zr–O bonds. It is clear that in the case of a 1:1 coverage with water molecules (i.e., one  $\text{H}_2\text{O}$  per Zr site) the zirconium atoms in the top layer would accomplish a full coordination.

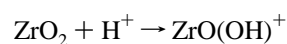
To assess the acidity of the surface hydroxyl groups we calculated the deprotonation energy, i.e., the energy required to remove a proton from a particular site and carry it to infinity.



This quantity, although purely hypothetical, can be calculated directly<sup>18</sup> and is a suitable measure of acidity for both gas-phase molecules<sup>22</sup> and surface sites.<sup>19</sup> It also allows for comparison with other solid acids such as zeolites.<sup>19</sup> It should be noted that when deprotonation energies are calculated, as well as proton affinities, discussed in the following section, periodic boundary conditions are applied, i.e., it is assumed that a proton is removed in every unit cell. No attempt was made to correct for the interaction of the proton with all its periodic images and to end up with a quantity for the isolated site. The deprotonation energies for the two bridging proton sites of the chemisorbed  $\text{H}_2\text{O}/\text{ZrO}_2(001)$  complex were calculated to be  $1456$  and  $1528$  kJ/mol. On the (101) surface deprotonation of both the physisorbed and chemisorbed  $\text{H}_2\text{O}$  complexes leaves either one terminal or one bridging surface hydroxyl group. The deprotonation energies are  $1553$  and  $1581$  kJ/mol, respectively. Hence, there is no appreciable difference between OH groups generated by water adsorption on the two types of Zr sites.

The corresponding results for terminal silanol groups<sup>20</sup> and for zeolite H-chabazite<sup>21</sup> are  $1400 \pm 25$  and  $1176$  kJ/mol, respectively. The OH groups on Zr(001) are thus significantly less acidic than bridging hydroxyls in zeolite H-chabazite, and even less acidic than terminal OH groups on silica.

However, as mentioned in the Introduction, the surface of zirconia comprises basic sites as well. As a surface hydroxyl group which was generated by protonation of a surface oxygen site can be considered as the conjugate acid of the latter base, we would expect this base to be quite strong. The calculation of the proton affinity of O atoms on the (001) surface, i.e., the energy change of the reaction



gave a value of  $-1170$  kJ/mol. Comparison with the gas-phase

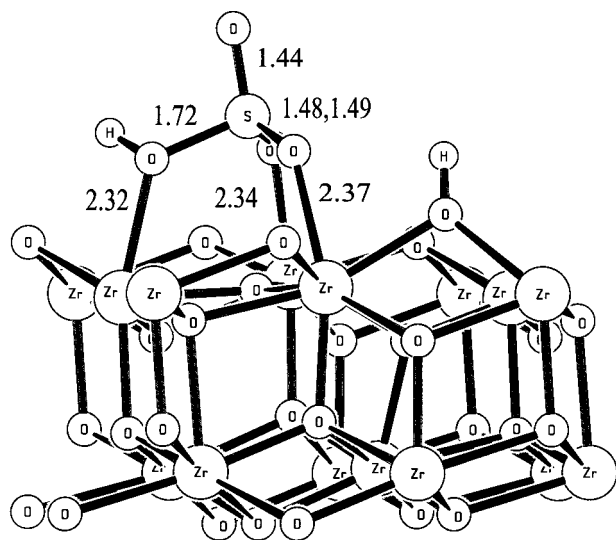


**Figure 5.** Equilibrium structure of the  $(\text{H}^+, \text{HSO}_4^-)/\text{ZrO}_2(101)$  adsorption complex (bond lengths in angstroms; only the two outermost  $\text{ZrO}_2$  layers are shown).

proton affinity of ammonia of  $-858 \text{ kJ/mol}^{22}$  shows that the surface oxygen atoms of pure zirconia are indeed strong basic sites.

**4.4. Structure of  $\text{H}_2\text{SO}_4$  on  $\text{ZrO}_2(101)$ .** This section presents the results of various structure relaxations of sulfuric acid adsorbed on a 5-layer slab model of the (101) surface of tetragonal zirconia. In our initial structure relaxations the starting configuration was a  $\text{H}_2\text{SO}_4$  molecule coordinated via its H atoms to the surface. A combination of standard geometry optimization techniques and short MD simulation runs at ambient temperature was applied to locate different stationary points on the potential energy surface. The first structure found was a hydrogen sulfate anion, i.e., one proton was abstracted by a nearby surface oxygen atom and a surface hydroxyl group was formed. Figure 5 shows the adsorption complex together with selected equilibrium bond lengths. The hydrogen sulfate ion forms three  $\text{Zr}-\text{O}$  bonds with the surface and contains three  $\text{S}-\text{O}$  single bonds and one  $\text{S}=\text{O}$  double bond. The interaction energy with respect to the isolated sulfuric acid molecule and the bare  $\text{ZrO}_2(101)$  surface is  $-243 \text{ kJ/mol}$ , which indicates a strong interaction dominated by electrostatics. The  $\text{Zr}-\text{O}$  bond lengths to the adsorbed anion are very close to those of the long  $\text{Zr}-\text{O}$  bonds in the bulk  $\text{ZrO}_2$  system, supporting the latter conclusion.

Nevertheless, in the second adsorption structure we find that the  $\text{H}_2\text{SO}_4$  molecule is completely dissociated and a sulfate anion and two surface hydroxyl groups have formed. Sulfuric acid is a strong polyprotic acid with a second acid constant about 100 000 times smaller than the first one.<sup>23</sup> Correspondingly, we calculated the first deprotonation energy to be  $1316 \text{ kJ/mol}$  and the second deprotonation energy to be  $3200 \text{ kJ/mol}$ . That sulfuric acid loses both protons on the  $\text{ZrO}_2$  surface again indicates the base strength of the surface oxygen atoms but also reflects the remarkably strong interaction of the sulfate ion with the surface zirconium atoms. Figure 6 shows the structure of the resulting adsorption complex. The only "free"  $\text{S}-\text{O}$  bond has a length typical of a  $\text{S}=\text{O}$  double bond ( $1.44 \text{ \AA}$ ), while the remaining three  $\text{S}-\text{O}$  bonds coordinated to surface Zr atoms have bond lengths of  $1.53 \text{ \AA}$  virtually equal to those calculated for an isolated  $\text{SO}_4^{2-}$  gas-phase anion ( $1.52 \text{ \AA}$ ). The adsorption energy of this complex is  $-322 \text{ kJ/mol}$ , i.e., it is by far more stable than the hydrogen sulfate surface complex. In a short molecular

dynamics simulation run at  $800 \text{ K}$  (a temperature typically applied to calcine the material), this structure proved stable and conversion to another possibly more stable structure was not observed.

Because White et al.<sup>11</sup> suggested that also sulfur trioxide may play a role as an active site, we optimized the structure of an  $\text{SO}_3$  molecule adsorbed on the (101) surface. Though an equilibrium structure could be found, its adsorption energy was repulsive, and this surface complex would not be thermodynamically stable.

**4.5. Structure of  $\text{H}_2\text{SO}_4$  on  $\text{ZrO}_2(001)$ .** In contrast to the (101) surface, on the (001) surface the initially adsorbed sulfuric acid molecule loses both of its protons at once and, thus, a hydrogen sulfate anion is not a stable surface species. Furthermore, after relaxation, an adsorption complex is obtained with the sulfate anion coordinated to the surface by only two of its oxygen atoms. However, Figure 7 shows that these two O atoms interact with four surface Zr atoms instead of interacting with just two as in the case of the (101) surface. This, of course, is due to the coordination number of the Zr atoms at this surface, 6 compared to 7 at the (101) surface, as already explained in section 4.2. Note that each of the two sulfate oxygen atoms binds to two Zr atoms in the same way as the oxygen atom of water. The calculated adsorption energy of  $-408 \text{ kJ/mol}$  is considerably higher than for a sulfate adsorbed on  $\text{ZrO}_2(101)$ . This stronger interaction is reflected in the calculated bond lengths of the anion as well. While two  $\text{S}-\text{O}$  bonds of double-bond character can be identified ( $1.44 \text{ \AA}$ ), the  $\text{S}-\text{O}$  bonds involved in surface interactions are by about  $0.1 \text{ \AA}$  longer ( $1.62 \text{ \AA}$ ) than those in the (101) sulfate complex.

So far we have found that sulfate anion complexes are the most stable surface sulfur species on tetragonal zirconia. The question which is intensively discussed in the literature, whether this sulfate anion is coordinated to the surface via two or three oxygen atoms, can now be answered if a specific crystallographic plane is considered. Figure 8 depicts the top view of the clean surfaces together with the adsorbed sulfate anion for the (101) (top) and (001) surfaces (bottom). It becomes immediately obvious why the preferred coordination of a tetrahedral sulfate species on a (101) plane is 3-fold. On this surface the zirconium atoms form an equilateral triangle with a side length of about  $3.6 \text{ \AA}$ , which makes a face-on coordination of the  $\text{SO}_4^{2-}$  tetrahedron possible. In contrast, on the (001) surface the Zr atoms are arranged as squares with a side length of  $3.6 \text{ \AA}$  and a diagonal of about  $5.1 \text{ \AA}$ . In this case only the edge-on configuration is possible, even if the two sulfate oxygen atoms would form an on-top coordination with two Zr atoms instead of the bridged coordination which allows for two more interactions.

Similarly as for the (101) surface, we checked for the (001) surface to determine if sulfur trioxide is a possible candidate of a surface sulfur species on zirconia. For comparison with the  $\text{H}_2\text{SO}_4$  adsorption structures found so far we initially adsorbed  $\text{SO}_3$  together with  $\text{H}_2\text{O}$  at the (001) plane and relaxed the structure. Surprisingly, a surface complex is found in which the S atom is 4-fold coordinated as in the sulfate species (Figures 9 and 10). This adsorption complex is actually very similar to that suggested by White et al.,<sup>11</sup> **1d**. The two oxygen atoms of  $\text{SO}_3$  interact in the same way with the surface as the above 2-fold coordinated  $\text{SO}_4^{2-}$  anion. Because of its Lewis acid character the sulfur atom forms an additional bond with a bridging surface oxygen atom. The additional water molecule was adsorbed dissociatively leading to two surface hydroxyl groups. The



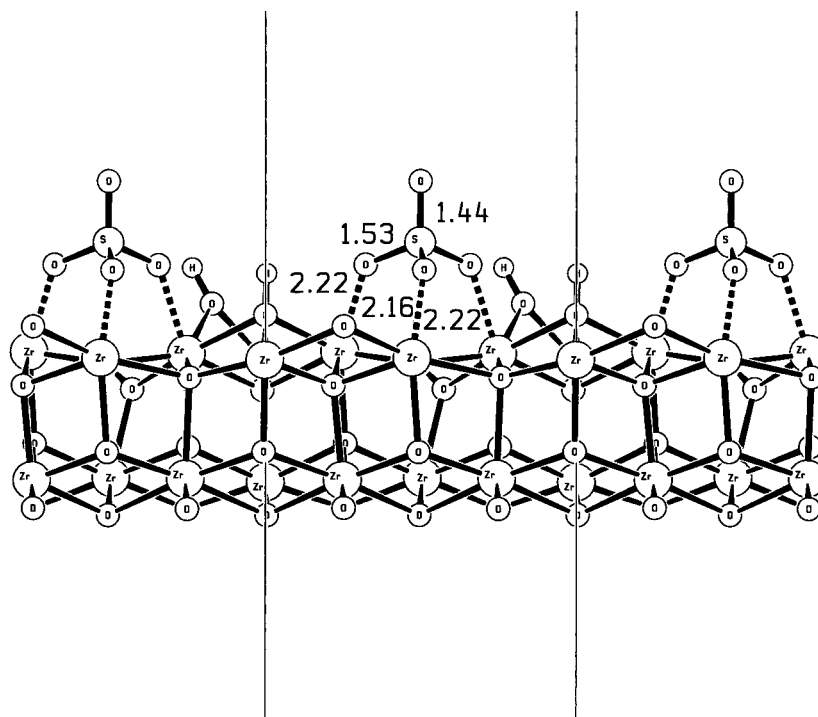


**Figure 6.** Equilibrium structure of the  $(2\text{H}^+, \text{SO}_4^{2-})/\text{ZrO}_2(101)$  complex with selected bond lengths in angstroms. The unit cell is translated in the  $+x$  and  $-x$  directions, and the  $c$  vectors ( $z$  axis) are indicated by two perpendicular lines.

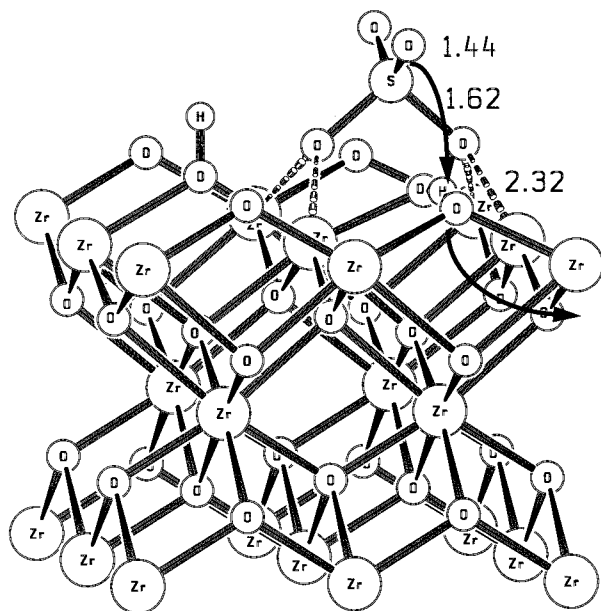


**Figure 7.** Equilibrium structure of the bidentate  $(2\text{H}^+, \text{SO}_4^{2-})/\text{ZrO}_2(001)$  adsorption complex. Only three  $\text{ZrO}_2$  layers from the full  $z$  dimension are shown. Typical bond lengths are given in angstroms.

adsorption energy is  $-467$  kJ/mol with respect to the clean zirconia surface and gas-phase  $\text{H}_2\text{SO}_4$ . While the calculated bond lengths of this surface complex resemble those of the (101) sulfate complex, it is considerably stronger bound than the latter.

**4.6. Vibrational Spectra.** In this section we present the vibrational frequencies calculated for the equilibrium structures of the four surface species (Table 4) and compare them with the available experimental data. The calculations are made within the harmonic approximation and are affected by systematic errors typical of the quantum mechanical method involved. Although for DFT results error cancellation is frequently observed, we make use of a simple scaling with a

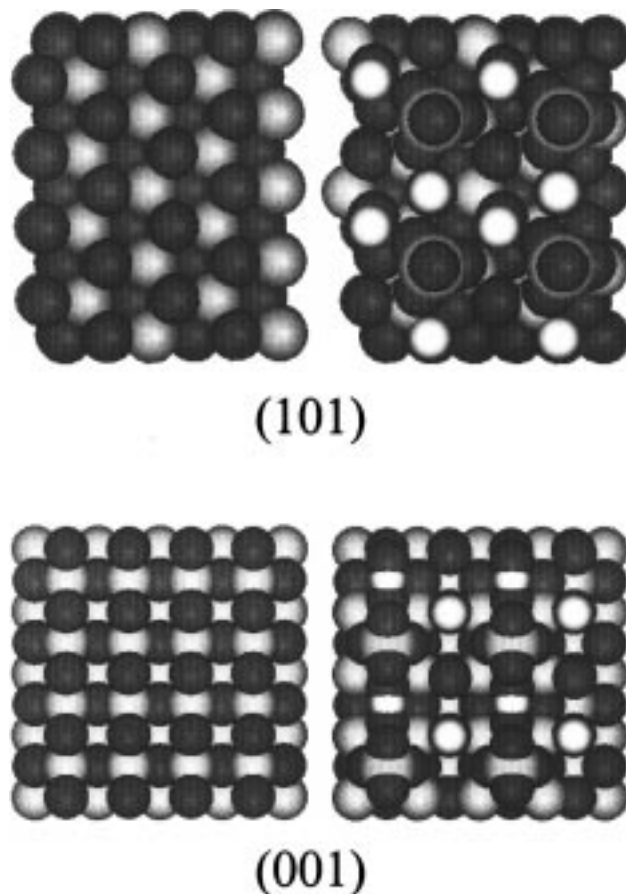


**Figure 8.** Top view of the surface unit cells (doubled in the  $x$  and  $y$  directions) of the clean (101) surface (top left), the tridentate  $(2\text{H}^+, -\text{SO}_4^{2-})/\text{ZrO}_2(101)$  complex (top right), the clean (001) surface (bottom left), and the bidentate  $(2\text{H}^+, \text{SO}_4^{2-})/\text{ZrO}_2(001)$  complex (bottom right). White spheres depict H atoms, light gray spheres indicate Zr atoms, dark gray spheres depict sulfur atoms, and dark spheres represent oxygen atoms.

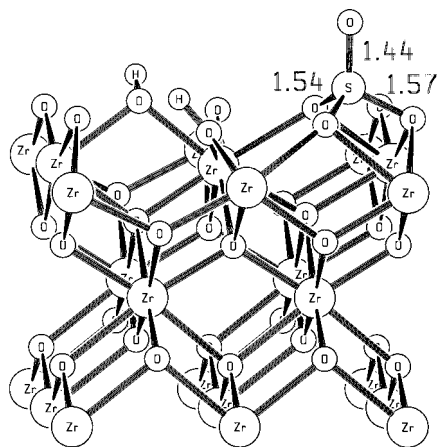


**Figure 9.** Equilibrium structure of the tridentate  $(\text{H}^+, \text{OH}^-, \text{SO}_3)/\text{ZrO}_2$ -(001) complex. Three  $\text{ZrO}_2$  layers are shown in the  $z$  direction. Bond lengths are in angstroms.

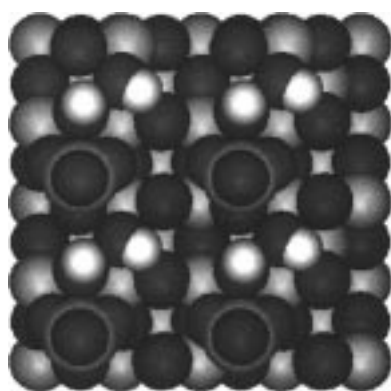


**Figure 10.** Top view of the (001) surface unit cell (doubled in the  $x$  and  $y$  directions) of the tridentate  $\text{SO}_3$  complex shown in Figure 9. (For description of atom types see Figure 9.)

**Table 4.** Harmonic Vibrational Frequencies ( $\text{cm}^{-1}$ ) in the  $\nu(\text{SO})$  Stretching Region Calculated for Different Adsorption Structures on the (101) and (001) Surfaces of Tetragonal Zirconia

	$\nu(\text{S}=\text{O})$	$\nu(\text{S}-\text{O})$
$(2\text{H}^+, \text{SO}_4^{2-})/\text{ZrO}_2(101)^a$	1375	1010, 978, 924
$(\text{H}^+, \text{OH}^-, \text{SO}_3)/\text{ZrO}_2(001)^b$	1425	1056, 1000, 943
$(2\text{H}^+, \text{SO}_4^{2-})/\text{ZrO}_2(001)^c$	1429, <sup>d</sup> 1344 <sup>e</sup>	1235, 967
$(\text{H}^+, \text{HSO}_4^-)/\text{ZrO}_2(101)^f$	1412	1221, 1056, 698

<sup>a</sup> Cf. Figure 6. <sup>b</sup> Cf. Figure 9. <sup>c</sup> Cf. Figure 7. <sup>d</sup> Asymmetric vibration. <sup>e</sup> Symmetric vibration. <sup>f</sup> Cf. Figure 5.

scale factor of 1.05.<sup>46</sup> It was assumed, e.g., by Bensitel et al.<sup>6</sup> or Morterra et al.,<sup>8</sup> that a  $\text{O}=\text{S}=\text{O}$  group as present in the bidentate sulfate species on the (001) surface exhibits an asymmetric stretch at about  $1400 \text{ cm}^{-1}$  and a symmetric stretch vibration in the range  $1250$ – $1150 \text{ cm}^{-1}$ . Our data (Table 4) support this assumption although we find a different assignment for the latter band. While the asymmetric stretching frequency

(44) Morterra, C.; Cerrato, G.; Pinna, F.; Signoreto, M. *J. Phys. Chem.* **1994**, *98*, 12373.

(45) Farcașiu, D.; Ghenciu, A.; Qi Li, J. *J. Catal.* **1996**, *158*, 116.

(46) Since it is known that the use of plane waves and pseudopotentials slightly deteriorates the quality of vibrational frequencies, we first tested the method for gas-phase sulfur trioxide. From experiments<sup>42</sup> the stretching frequencies were determined to be  $1391 \text{ cm}^{-1}$  (doubly degenerated) and  $1065 \text{ cm}^{-1}$ . With our method we obtained 1330 and  $1000 \text{ cm}^{-1}$ , which means that experimental frequencies are underestimated by about 5%. To correct for this red shift, all calculated frequencies are scaled by a factor of 1.0526. It should be noted that this crude scaling accounts for both systematic errors of the calculated harmonic force constants and neglected anharmonicity effects.

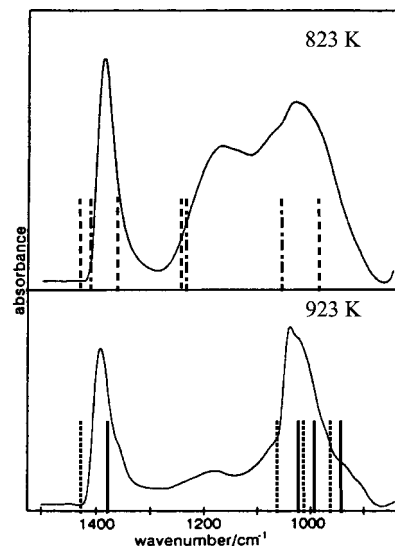


**Figure 11.** Experimental IR spectrum<sup>8</sup> (top, tetragonal SZ calcined at 823 K; bottom, tetragonal SZ calcined at 923 K) together with the stick spectrum of the calculated vibrational frequencies scaled by 1.05.<sup>46</sup> Solid lines: tridentate  $(2\text{H}^+, \text{SO}_4^{2-})/\text{ZrO}_2(101)$ . Dashed lines: bidentate  $(2\text{H}^+, \text{SO}_4^{2-})/\text{ZrO}_2(001)$ . Dotted lines: tridentate  $(\text{H}^+, \text{OH}^-, \text{SO}_3)/\text{ZrO}_2(001)$ . Dashed-dotted lines:  $(\text{H}^+, \text{HSO}_4^-)/\text{ZrO}_2(101)$ .

closely approaches the observed frequency, the symmetric stretch ( $1344 \text{ cm}^{-1}$ ) is about  $90 \text{ cm}^{-1}$  higher and thus appears closer to the symmetric stretch in the spectrum as predicted by experimental studies. Instead our calculations predict the asymmetric S–O stretch frequency ( $1235 \text{ cm}^{-1}$ ) to appear within the frequency range where the symmetric S=O stretch frequency is assumed. Furthermore the above authors conclude that the presence of just one S=O bond, as is the case in the two 3-fold coordinated adsorption complexes, gives rise to a S=O stretching band at about  $1400 \text{ cm}^{-1}$  which is separated by  $300$ – $400 \text{ cm}^{-1}$  from the S–O stretching vibrations. Our calculated frequencies also support this assumption. In both tridentate complexes, the calculated separation amounts to  $350 \text{ cm}^{-1}$  and matches the observed gap.

Figure 11 shows an experimental IR spectrum of Morterra et al.<sup>8</sup> together with our calculated frequencies. We also show the frequencies of the hydrogen sulfate form of  $\text{H}_2\text{SO}_4/\text{ZrO}_2$ -(101) complex (dashed-dotted sticks). The latter structure, though significantly less stable than the sulfate structures, may also contribute to the experimental spectrum of samples calcined at lower temperatures. As is evident from Figure 11, the stick spectrum predicted for the tridentate sulfate and  $\text{SO}_3$  species on the (101) and (001) surfaces, respectively, with the wide gap of about  $350 \text{ cm}^{-1}$  fitted the experimental spectrum recorded after calcination at 923 K. At this point it can be concluded that heating zirconia up to a sufficiently high temperature in the presence of  $\text{SO}_3$  should lead to a spectrum as shown at the bottom of Figure 11. To our knowledge this was only done for  $\text{Fe}_2\text{O}_3$  and at a significantly lower calcination temperature.<sup>2</sup> The stick spectrum calculated for the (101) hydrogen sulfate and bidentate (001) sulfate species with additional bands in the  $1200 \text{ cm}^{-1}$  region matches the spectrum recorded for samples calcined at a lower temperature, 823 K.

Interestingly Bensitel et al.,<sup>6</sup> who studied the monoclinic phase of SZ,<sup>7</sup> arrived at the same conclusion in that they also favored a 3-fold coordinated surface complex. This indicates that on the surface of monoclinic sulfated zirconia this configuration is the prevailing sulfur species and causes a similar IR spectrum as is done on the surface of the tetragonal phase. However, as was found by Morterra et al.,<sup>8</sup> the spectrum in the



range 1100–900  $\text{cm}^{-1}$  is more complex, indicating that more structures, possibly at different crystallographic surfaces, are present.

**4.7. General Discussion.** Morterra and co-workers<sup>8</sup> observed interesting changes in the IR spectra when going from a SZ sample calcined at 673 K to one calcined at 923 K. They concluded that the structure present at the surface of the sample calcined at the lower temperature is transformed into another structure without any decline in the overall concentration of sulfate groups. In agreement with this observation we found two structures on the (001) surface, bidentate  $\text{SO}_4^{2-}$  and tridentate  $\text{SO}_3$ . To prove the above assumption of Morterra et al. it remains to show whether and how it is possible to transform the less stable structure into the second more stable one, in other words, whether it is possible to simulate the calcination process. For this purpose we performed an MD simulation at a temperature of 800 K, slightly above the temperature at which Morterra et al. observed that the IR spectra began to change (776 K). As the initial structure, the 2-fold coordinated sulfate anion on the (001) surface was chosen. The simulation time was 2 ps after an equilibration period. In fact, after about 1.5 ps this initial structure was transformed into the 3-fold coordinated  $\text{SO}_3$  complex we had identified as the most stable form on the (001) surface. To accomplish this the surface had to reconstruct. As can be seen from Figure 7, the top layer of the (001) surface consists of oxygen atoms which are arranged as rows parallel to each other and bridge the underlying Zr atoms. To achieve a 3-fold coordinated configuration one of these top-layer O atoms moved out of the row and created a Zr–O–Zr bridge orthogonal to it. Then one of two noninteracting oxygen atoms of the sulfate anion moved down and restored the O-atom point defect in the row. Finally the sulfate anion accomplished the same face-on coordination as the sulfate group on the (101) surface.

On the basis of our calculated vibrational frequencies it is now possible to explain the spectral changes observed by Morterra et al.<sup>8</sup> when the material was calcined at temperatures higher than 773 K. The authors found that in the 1250–1130  $\text{cm}^{-1}$  interval a broad band is present in samples calcined up to temperatures of 823 K (Figure 11, top). Two frequencies lie in this interval: one at 1235  $\text{cm}^{-1}$  calculated for the bidentate sulfate anion on the (001) surface and another at 1221  $\text{cm}^{-1}$  calculated for the hydrogen sulfate complex on the (101) surface (see Table 4). After calcination at temperatures above 773 K, the group of bands in the above-mentioned interval starts to disappear and the spectrum of the sample calcined at 923 K exhibits just two sharper peaks at about 1400 and 1040  $\text{cm}^{-1}$  (Figure 11, bottom). We can now lend further credit to their assumption that this is due to a conversion from one or more thermodynamically unstable structures to another stable structure. Above we showed that by an MD simulation at 800 K a transition from the 2-fold to the 3-fold coordinated (001) surface complex accompanied by a reconstruction in the oxygen top layer can be achieved. This allows us to conclude that at the surface of samples calcined at temperatures of about 900 K only one configuration is present, a tridentate sulfate anion on the (101) surface and a tridentate  $\text{SO}_3$  complex on the (001) surface. Figure 12 summarizes the relative stabilities of the different surface species found. It also shows that it is easier to dehydrate SZ leaving  $\text{SO}_3$  on the (001) surface than to remove  $\text{SO}_3$  from a hydroxylated surface.

An enhanced electron-accepting ability of zirconium atoms involved in interactions with sulfate groups was assumed to render Brønsted sites in the vicinity of such Zr sites more acidic

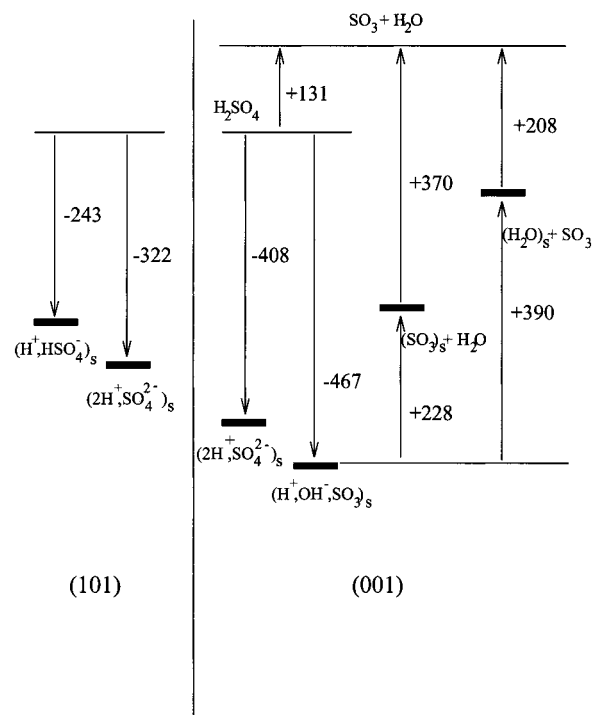


**Figure 12.** Schematic representation of the total energies of different surface complexes localized in this work.

or even superacidic.<sup>17</sup> We are now in a position to check whether this effect actually takes place by calculating the deprotonation energies. We did this for the (001) tridentate  $\text{SO}_3$  complex and compared the values obtained with those for the pure hydroxylated (001) surface presented in section 4.3. The calculations yielded values of 1486 and 1522 kJ/mol, which are very close to the deprotonation energies of the pure zirconia surface of 1456 and 1528 kJ/mol. No appreciable change in these energies upon sulfation of the surface can be seen which contradicts the assumption above. A further hypothesis supported by some authors is that the Brønsted sites of SZ are somehow connected to the sulfate species, i.e., protons coordinated to sulfate ions. Such a species would be the hydrogen sulfate anion we found on the (101) surface. Although its deprotonation energy of 1354 kJ/mol is about 100 kJ/mol lower than the value calculated for the strongest site so far, it is still higher by about 150 kJ/mol than the value of H-chabazite.

These acidity predictions are in line with studies of Drago et al.<sup>4</sup> and Adeeva et al.,<sup>5</sup> who challenged the hypothesis of superacidity. Drago et al. combined information from calorimetry and adsorption of pyridine onto the solid acid and concluded that the acidity of SZ is lower than that of zeolite HZSM-5 and comparable to that of zeolite HY. Adeeva and co-workers arrived at the same conclusion by analyzing the changes in the NMR and IR parameters caused by adsorption of acetonitrile. We are aware of the fact that the Brønsted sites modeled in our calculations are only representative of rather abundant protonic sites on regular surfaces. From experimental studies it is known that the concentration of Brønsted sites on the surface of SZ calcined at 900 K is very small.<sup>44</sup> These types of Brønsted sites may be located at defects or on less stable surfaces and are thus not accessible with the slab models used in our calculations. However, it is not yet clear whether Brønsted acidic sites are involved at all in the catalytic process over SZ.<sup>45</sup>

## 5. Conclusions

We have shown that the crystal faces that are favorably exposed by the tetragonal phase of zirconia are (101) and (001)

in this order. On those two surfaces sulfuric acid deprotonates completely, leading to an adsorbed sulfate anion and surface hydroxyl groups. Hydrogen sulfate groups are by far less stable and seem not to be present at ambient temperatures. The most stable configurations are a sulfate anion 3-fold coordinated to surface Zr atoms on the (101) surface and an  $\text{SO}_3$  complex also 3-fold coordinated (to 2 Zr atoms and 1 O atom) on the (001) surface. Because the surface Zr atoms on the (001) surface lack one more coordination compared to the (101) surface, the former interact significantly more strongly with sulfuric acid. The adsorption energy of the (001)  $\text{SO}_3$  complex of  $-467$  kJ/mol is higher by more than 140 kJ/mol than that of the (101) sulfate anion. A bidentate sulfate anion on the (001) surface is thermodynamically not stable at a temperature of 800 K. It is transformed into the 3-fold coordinated form accompanied by a reconstruction of the oxygen top layer in the course of which an oxygen atom moves from one Zr–O–Zr bridge to a neighboring bridge and in this way creates the space needed to form a third coordination of the sulfate anion.

The experimentally derived IR spectra can be explained by the presence of sulfate anions on both crystallographic planes studied in this work. For the 3-fold coordinated configuration a spectral splitting of  $350\text{ cm}^{-1}$  between the  $\nu(\text{S}=\text{O})$  and  $\nu(\text{S}-\text{O})$  stretching bands is predicted, which is well in agreement with experimental IR spectra. This splitting is much lower in the 2-fold coordinated configuration in which the asymmetric and symmetric coupled  $\nu(\text{S}=\text{O})$  vibrations are separated by only about  $90\text{ cm}^{-1}$ , again in line with experimental evidence. Furthermore the change in the IR spectrum of tetragonal SZ

observed when going to a higher calcination temperature can be explained by the transformation of the 2-fold to a 3-fold coordinated sulfate complex on the (001) crystal face. Therefore at the surface of the catalytically active material the 3-fold coordinated sulfate complex should be the prevailing sulfur species. We cannot exclude that on other planes or possibly at defect sites other structure types are present, though.

The surface of pure zirconia is a strong base. It is therefore not surprising that a strong acid like sulfuric acid completely dissociates on the zirconia surface, giving a sulfate anion. As long as strong basic sites are accessible, deprotonation occurs and no stronger acid than surface hydroxyl groups can exist on the zirconia surface. From the deprotonation energies of the types of Brønsted sites that were modeled in our calculations, we conclude that even after sulfation these sites are less acidic than those of zeolites. Therefore the unique catalytic activity cannot be related to its acidity but must possibly be interpreted in terms of reduction–oxidation reactions.<sup>45</sup>

**Acknowledgment.** The authors thank Prof. M. Parrinello (MPI für Festkörperforschung Stuttgart) for making available the CPMD program. F.H. thanks Dr. J. Hutter (MPI FK Stuttgart) for many valuable hints and support in using the CPMD program. We are grateful to the Höchstleistungsrechenzentrum (HLRZ) at the Forschungszentrum Jülich for a generous grant of computer time at their CRAY T3E machines. This work was supported by the “Max-Planck-Gesellschaft” and by the “Fond der Chemischen Industrie”.

JA9825534